Issue: 8 2025
e-ISSN:2717-8277
International Journal of Water Management and Diplomacy

Seepage Control of Irrigation Water:

A Critical Constituent in Disaster Avoidance and Loess Project Management

Serges Mendomo Meye*[1], Paul Fabrice Nguema[1], Tchamake Fomeza Michelle Princesse[1], Engueno Awono Serge[1]
Correspondence Author, e-mail: sergesmendomo@yahoo.fr

Abstract:
Water penetration in loess slopes has a notable impact on the physical and mechanical attributes of the soil. Within loess landscapes, certain pathways are favored for water seepage, highlighting the necessity of investigating preferential flow to grasp the water seepage process in loess. The identification of cracks, particularly microscale cracks, is facilitated through the utilization of electrical resistivity tomography and geological radar techniques. Furthermore, to monitor the seepage process, an in-situ single-ring infiltrometer test is performed in the hidden fracture locations. The findings from these on-site tests serve as the basis for developing both a single-seepage model and a dual-seepage model, which aim to replicate the seepage process occurring in the preferential channel. For engineering purposes, the examination of a landslip that occurred at the rear edge of most loess plateau is underway. Within the numerical framework, two types of irrigation conditions are simulated: high intensity with short duration and low intensity with extended duration. In instances of high-intensity irrigation, the preferential flow rate takes precedence and exerts a beneficial effect on seepage. Rapid infiltration of irrigation water occurs in the deep soil, causing groundwater levels to rise, while the top matrix region remains devoid of saturation. In instances of low intensity, matrix flow takes precedence, resulting in a saturated seepage condition. Seepage control of excessive irrigation water plays a crucial role in disaster prevention and the effective management of loess projects.

Keywords: Hidden Crack; Preferential Channel; Seepage Process; Dual-Seepage Model; management of loess projects; seepage control of irrigation water

[1] *Higher Institute of Agriculture, Forestry, Water Resources, and Environment, Department of Hydraulic and Water Sciences Technology, University of Ebolowa, Ebolowa- Cameroon.*

HPA January 15 2025

1. Introduction

1.1 Research significance

The management of water has emerged as a critical factor in disaster prevention and the effective execution of loess projects. To avert the calamitous consequences of water-induced loess, engineers must initially delve into the mechanisms through which water infiltrates the loess. The natural loess slope is riddled with numerous fractures, including concealed cracks that remain hidden beneath the surface. Unfortunately, these buried cracks are often disregarded in irrigation activities and the design of water control systems for engineering purposes. The preferred routes for water seepage on engineered slopes encompass the boundaries formed by filling and excavation, cracks resulting from unloading, and subterranean pipelines. Water within these preferential channels can swiftly permeate to the lower layers, thereby underscoring its significance in water control for engineering purposes. Consequently, it is imperative to thoroughly investigate the seepage characteristics of water within these dominant channels.

A considerable number of countries around the world exhibit the prevalent loess distribution region (P. Li. and Q. Hui, (2018)). However, the increase in human endeavors like city expansion, industrial growth, and energy consumption has escalated the need for water, causing pollution in both land and water resource (P. Li. and Q. Hui, (2018), P.Li, H. Qian, K. Howard and J. Wu,(2015), E. Saibaba Reddy, K. Rama Sastri et K. Bhaskar ,(2010)) . Consequently, the loess plateau is currently confronted with significant challenges in terms of water resource development and environmental preservation. A thorough comprehension of the properties of loess and a comprehensive understanding of the current water resources situation in the loess plateau area are of utmost importance (W. Shao, T. Bogaard and M. Bakker,(2015) , P. Li. and Q. Hui, (2018)) .

Water serves as a fundamental element for driving economic development and safeguarding the environment in the loess plateau on a global scale. The loess plateau grapples with the formidable environmental challenges of drought and water scarcity, which have profound implications for the advancement of ecological civilization and economic growth (P. Li. and Q. Hui, (2018) , I. Smalley, S. Marković and Z. Svirčev,(2011) , P. Garcia-Chevesich, X. Wei, J. Ticona and G. Martínez,(2020)) . River water and groundwater are the predominant water resources harnessed in research field, catering to diverse needs and applications. As per the available literature, the water supply in the research region is predominantly reliant on river water, which contributes to a substantial 77.3% of the total. In contrast, groundwater plays a comparatively smaller role, accounting for 22.7% of the overall water resources (I. Smalley, S. Marković and Z. Svirčev,(2011), P. Li. and Q. Hui, (2018)). In the loess plateau, the main utilization of river water revolves around agricultural irrigation and industrial production. However, for domestic water supply, the primary reliance is on groundwater(P. Garcia-Chevesich, X. Wei, J. Ticona and G. Martínez,(2020)) .

The region frequently experiences irrigation-induced landslides, which can be attributed to the seepage of water through surface fissures and sinkholes (Y. Liang, J. Qiao and C. Xie, (2019) , L. Zhu, J. Hu and J. Jia(2013), J. Dong, (2017) , P. Garcia-Chevesich, X. Wei, J. Ticona and G. Martínez,(2020)). Not only does irrigation play a role in triggering landslides in this area, but the occurrence of a landslide can also increase the likelihood of additional landslides happening subsequently, as demonstrated in studies conducted in the Jiaojiayatou region of the People's Republic of China (J. Jia, L. Zhu and W. Hu (2013)) .Studies have uncovered a distinct relationship between variations in groundwater table levels (as a result of agricultural irrigation) and the history of landslides (P. Garcia-Chevesich, X. Wei, J. Ticona and G. Martínez,(2020) , Y. Dong, P. Sun, M. Zhang, X. Cheng and J. Bi,(2013)). The Heifangtai loess plateau has witnessed water table elevations surpassing 20 meters for over four decades in specific locations, as reported by Zhang (M. Zhang,(2013)) in their study. Xu et al.(L. Xu, F. Dai, X. Tu, L. Tham, Y. Zhou and J. Iqbal,(2013)) projected an annual rise of 0.18 m in the aforementioned region. Additionally, Xu et al.(L. Xu, F. Dai, L. Tham, X. Tu, H. Min and Y. Zhou, (2011)"). executed a model to evaluate the water-related impacts of watering on the stability of a loess face face at Heifangtai (G.-C. Pablo et al 2021).

Their findings revealed that the establishment of extensive agricultural fields played a pivotal role in triggering persistent landslides within this geological formation. Irrigation's effect on the stability of the loess terrain was also investigated on the Heifangtai Plateau.(Gu et al.2018), in independent research efforts, along with the study by Wu et al. (W. Wu, X. Su and X. Meng,(2014)) ,both studies concluded that the primary cause of recent landslides in the area was the surplus water generated from agricultural irrigation methods. These findings align with the conclusions drawn by Hou et al 2018. regarding the instability of the Heifangtai platform, as well as the research conducted by Duan et al. (2019) on the instability of the Jingyang loess platform situated in the northern Chinese province of Shaanxi (P. Garcia-Chevesich, X. Wei, J. Ticona and G. Martínez,(2020)). Li and Jin (2012) conducted an analysis in the same region and investigated the initial stage of deep landslides. Their findings indicated that the primary factor triggering these landslides was the rise in water tables, which was attributed to the extensive irrigation activities. Similarly, Gu et al.(2015) Gao et al. (2019), and Qui et al. (2019) reached comparable conclusions in their respective studies on landslides in Gansu, Sichuan, and Wuhai provinces.
Extensive scholarly research has been conducted to explore the strategies employed in determining and altering the seepage coefficient in different scenarios, which serves as a key parameter for evaluating soil seepage (B. Zhou and Z. Chen(2019), H. Hu (2018)). The findings reveal that the seepage coefficient of Malan loess experiences a substantial decrease from saturated to unsaturated conditions, declines with an increase in dry density, and eventually stabilizes (B. Hong, X. Li and G. Chen(2016), , T. Wang, T. Yang and J. Lu (2016, K. Zhao, Q. Xu and X. Zhang (2018)). The configuration of loess can be scrutinized to comprehend the mechanisms of water seepage. The seepage of water within loess

materials is a complex phenomenon. Several investigations have been carried out on the seepage behavior of water flow in loess (J. Lu and and B. Chen (2007), T. Wang, N. Li and D. Xie (2004)) ,the relationship between soil and water (P. Li, T. Li and A. Wang (2013)) , and the water retention properties through field seepage tests and laboratory experiments (Q. Mu, Y. Dang and Q. Dong (2019),). Some researchers suggest that vertical loess joints play a significant role in surface water seepage, along with pore seepage. Ground fissures and sinkholes are highlighted as the main channels through which surface water flows (L. Xu, H. Li and D. Wu(2008)).

In the study of water field simulation in loess, researchers have examined various aspects such as the water field of unsaturated loess subgrade (T. Wang (2008)) , pore flow modeling method, and pore velocity distribution(Y. Liang(2011),). Moreover, investigations have been carried out on the three-dimensional seepage of loess landslide drainage system (A. Zhang, S. Kang and P. Li(2004),), coupling analysis of phreatic seepage field and slope stability in Heifangtai irrigation area (P. Sun, M. Zhang and Y. Dong (2013),), and pore flow characteristics of porous media using transparent soil technology (Y. Liang, P. Chen and J. Lin (2019),) . The numerical simulation of seepage under the combined influence of preferential flow and matrix flow has been investigated by several researchers (E. Saibaba Reddy, K. Rama Sastri et K. Bhaskar ,(2010)) .The seepage of water is influenced by the presence of a preferential channel, leading to the need for studying this phenomenon (W. Shao, T. Bogaard and M. Bakker,(2015) , T. Vogel, H. Gerke and R. Zhang (2000)).

Considerable advancements have been achieved in studying the infiltration of water in loess. However, the emphasis has primarily been on laboratory tests conducted on remoulded soil, neglecting the complexities of soil in the field. While the exploratory well sensor monitoring method is frequently employed for field experiments, it fails to accurately depict the in-situ two-dimensional seepage process. The seepage characteristics of water in the preferential channel of loess were explored by utilizing the rear edge landslip on a loess plateau as a test site. Through field seepage testing and numerical simulations that did not disturb the site, the seepage behavior of water in the preferential channel of loess was investigated. These findings could potentially lay the groundwork for water management strategies and disaster mitigation measures on the loess plateau.

1.2 What is the challenge we are addressing and what incentivizes us to pursue this research?

Prior to 1967, the mountainous area being examined, which encompasses 13.7 km^2, was unpopulated (X. Hou, S. Vanapalli and T. Li (2018),). In order to facilitate dam construction, inhabitants of the reservoir region were resettled to the loess highland, where they engaged in farming practices. In response to farming needs, a multitude of irrigation canals have been established over time, featuring the ability to extract water from the main river through pumping mechanisms. The collective area covered by these irrigated lands is approximately 7.53 km^2 (L. Xu, F. Dai, L. Tham, X. Tu, H. Min and Y. Zhou, (2011, X. Hou,

S. Vanapalli and T. Li (2018),). In the 1980s, the annual irrigation water volume per unit area was recorded at about 0.89 m^3, which then dropped to 0.64 m3 in the 1990s. Despite the region experiencing relatively low yearly precipitation levels, ranging from 316 mm/a to 400 mm/a, the annual evaporation rate remains high at around 1568 mm/a. The substantial impact on the natural hydraulic balance is attributed to irrigation water.
The escalation of groundwater levels in the region resulted in over 70 landslides (Fig. 1(b)), attributed to the prolonged use of flood irrigation for agricultural activities. Despite the significant impact of irrigation-induced landslides, traditional flood irrigation methods persist, especially in areas characterized by multiple cracks along the plateau's periphery. The field harbors a plethora of concealed fractures that reach into the plateau, thereby facilitating the unhindered infiltration of irrigation water into the soil. Field investigations, field monitoring, and indoor experiments are employed in this study to develop a single-seepage model and a dual-seepage model that replicate the seepage process within the designated channel. The research focuses on investigating the seepage characteristics of water in the presence of concealed cracks by utilizing the back edge of the #CH7 landslip as a field test area (Fig. 1(a)).

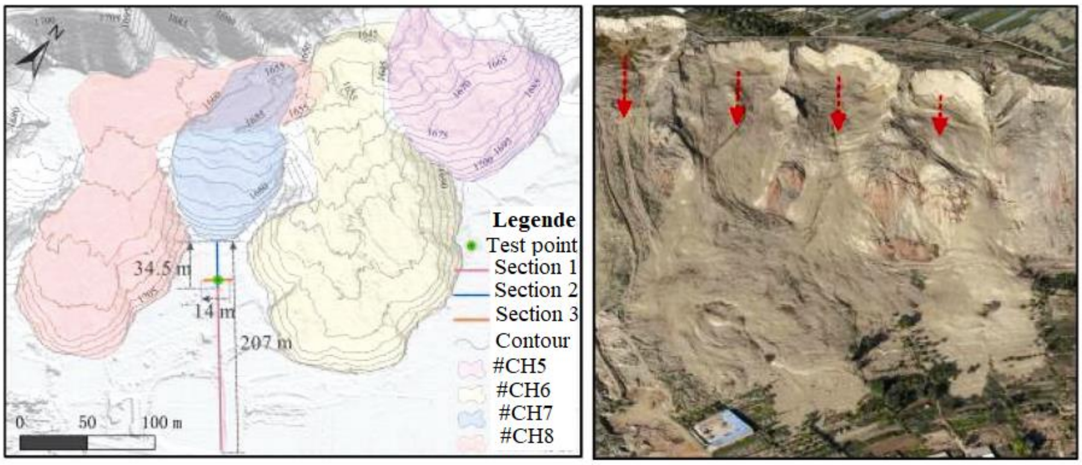

(a) Field test section **(b) Landslide due to flood irrigation**

Fig. 1 Overview of the research environment

2. Materials and methods

2. 1 Seepage model

The numerical simulation in the Fluid Flow module of COMSOL software relies on the adoption of the Richards equation. In order to effectively simulate the role of the preferential flow domain in the seepage process, the single seepage model, referred to as the single Richards equation, is initially employed for calculating the seepage characteristics exclusively in the case of matrix flow. Following this, the dual seepage model incorporates two Richards equations, specifically Eqs. (1) and (2), which are able to undergo conversion and interplay with one another (H. Gerke. and M.Genuchten(1993),). The water mass exchange coefficient, as defined by Eqs. (3) and (4) in reference (C. Ray, T.

Ellsworth and A. Valocchi (1997)), is employed to characterize the seepage behavior in situations where both the flow domain and matrix domain are present simultaneously. The section where the flow domain extends allows for the dispersion of water into the adjacent soil surrounding the channel domain. This altered water will travel as matrix flow, thereby promoting a faster seepage through the underlying layers.

$$\left[C_f + \Theta_f S_s\right]\frac{\partial h_f}{\partial_t} = \nabla\left[K_f\left(\nabla h_f + \nabla_z\right)\right] - \frac{\Gamma_w}{w_f}, \quad (1)$$

$$\left[C_m + \Theta_m S_s\right]\frac{\partial h_m}{\partial_t} = \nabla\left[K_m\left(\nabla h_m + \nabla_z\right)\right] + \frac{\Gamma_w}{w_m}, \quad (2)$$

$$\Gamma_w = \alpha_w K_a\left(h_f - h_m\right), \quad (3)$$

$$K_a = \frac{K_f + K_m}{2}, \quad (4)$$

In the given formula, the subscripts *f* and *m* are assigned to represent the preferential flow and matrix flow respectively. $C(L^{-1})$ is used to denote the water content, while Θ *(1)* signifies the soil saturation. The variables h *(L)*, $t(T)$, and z represent the head height, time, and vertical coordinate respectively. Additionally, $K(LT^{-1})$ stands for the isotropic hydraulic conductivity, $Ss(L^{-1})$ indicates the unit volume water capacity, and w *(1)* represents the volume proportion. Furthermore, $\Gamma_w(T^{-1})$ is the water exchange coefficient of the two equations, $\alpha_w(L^{-2})$ denotes the water conversion rate, and $K_a(LT^{-1})$ signifies the average hydraulic conductivity of the two models (B. Arora, B. Mohanty and J. Mcguire (2011) , H. Laine-kaulio, S. Backnas and T.Karvonen (2014) , W. Shao, T. Bogaard and M. Bakker,(2015)).

The total volume ratio of the two models is equivalent to 1.

$$w_f + w_m = 1, \quad (5)$$

The overall volumetric water content of the soil is the median volumetric water content of the two simulations.

$$\theta = w_f\theta_f + w_m\theta_m; \quad (6)$$

Likewise, the complete hydraulic conductivity of the soil can be calculated.

$$K_s = w_f K_{sf} + w_m K_{sm}; \quad (7)$$

In accordance with this, the initial fixed flow assigned to the model can be apportioned to each model.

$$i = w_f i_f + w_m i_m. \quad (8)$$

The Brooks-Corey function simultaneously characterizes the matrix and preferential flow domains (R. B. a. A. Corey (1964), T. Bogaard and M. Bakker,(2015) , S. Wei , B. Thom , S. Ye et . B. Mark (2016)).

$$\Theta = \frac{\theta - \theta_r}{\theta_s - \theta_r} = \begin{cases} \left|\alpha_{BC} h\right|^{nBC} & \left(\alpha_{BC} h < -1\right) \\ 1 & \left(\alpha_{BC} h \geq -1\right) \end{cases}, \tag{9}$$

$$K = K_s \Theta^{2/n_{BC} + l_{BC} + 2} = K_s \left|\alpha_{BC} h\right|^{-2-n_{BC}\left(l_{BC}+2\right)}, \tag{10}$$

$$C = -\frac{d\theta}{d\left|h\right|} = \begin{cases} \alpha_{BC} n_{BC} \left(\theta_s - \theta_r\right) \left|\alpha_{BC} h\right|^{-n_{BC}-1} & \left(\alpha_{BC} h < -1\right) \\ 0 & \left(\alpha_{BC} h \geq -1\right) \end{cases}, \tag{11}$$

The formula incorporates various elements. The volumetric water content is represented by $\Theta(L^3L^{-3})$, with the subscripts s and r indicating the saturated and residual water content respectively. The saturated seepage coefficient is denoted as K_s (LT^{-1}), while the parameters α_{BC}, l_{BC}, and n_{BC} are employed for curve fitting, considering the qualities of the soil and water.

2. 2 Boundary conditions

The geometric dimensions of the numerical simulation are 3 meters wide and 2 meters high, with the upper 1 meter consisting of unsaturated loess, when combined with the field test results. To capture the effects of the seepage domain of the upper unsaturated loess on the moisture content of the lower soil layers, the numerical simulation in Fig. 2 designates the bottom 1 m as saturated loess. The change in the bottom saturated layer can be evaluated when a flow domain is present. The left, right, and lower boundaries are characterized as non-flow boundaries, with the top boundary allowing for seepage flow. Research indicates that Heifangtai practices flood irrigation, with a specific intensity of around 25 mm/h during irrigation sessions.

These sessions typically last for close to 4 hours and are conducted approximately 8 times throughout the crop growth cycle. Thus, within the numerical simulation, a high-intensity irrigation rate of 25 mm/h was designated, with a simulation duration of 32 hours. To contrast the simulation results between high and low intensity, a low-intensity irrigation rate of 2 mm/h was employed, with a simulation duration of 400 hours. The total irrigation volume in both scenarios remains unchanged.

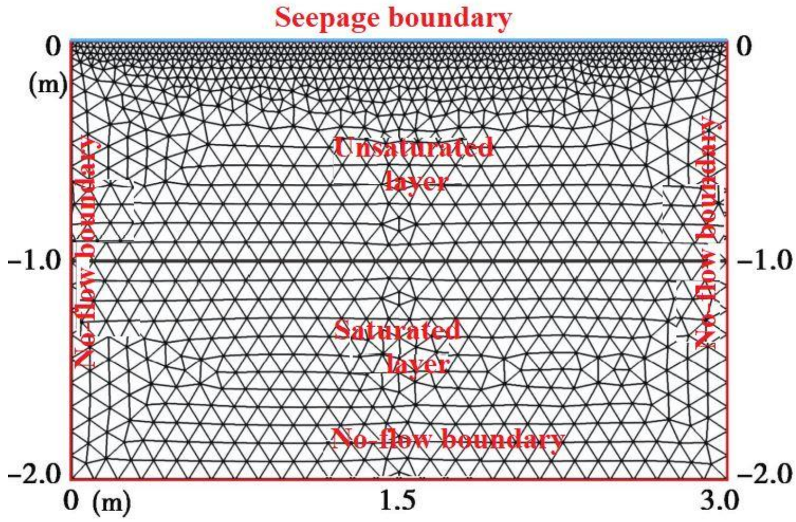

Figure 2 Computational mesh and boundary conditions

2.3 Parameter selection

The flow domain in the soil is characterized by a sparse distribution of channel domains, resulting in a volume ratio wf of 0.1. In the single-seepage model, the hydraulic conductivity K_s remains consistent with that of the flow domain. However, in the dual-seepage model, K_s is adjusted by the volume ratio to account for both matrix flow and the flow domain. The determination of K_s is achieved via a single ring test. Reference (W. Shao, T. Bogaard and M. Bakker,(2015)). provides data on the water conversion coefficient α_w, as well as the Brooks Corey fitting parameters α_{BC}, l_{BC}, n_{BC}, which delineate the relationship between substrate flow and flow domain. Table 2 provides a detailed description of these particular criteria.

Table 1. Parameter Details

Symbol	Designation	Numerical value
θ_s	Saturated water content	0.4
θ_r	Residual water content	0.04
K_s	Saturated seepage coefficient/(cm·h^{-1})	2.56
K_{sf}	K_s/(cm·h^{-1}) of dominant flow	23.49
K_{sm}	K_s/(cm·h^{-1}) of matrix flow	0.2349
α_w	Water conversion coefficient/m^{-2}	0.2
α_{BC}	Brooks-Corey fitting parameters/cm^{-1}	0.068
n_{BC}	Brooks-Corey fitting parameters	0.322
l_{BC}	Brooks-Corey fitting parameters	1

3. Results and discussion

3.1 Two-dimensional seepage characteristics

In the field seepage test, a constant water head is applied to mimic high-intensity irrigation practices. The numerical simulation incorporates two simulation conditions: high-intensity irrigation and low-intensity irrigation. The distribution of effective saturation in a two-dimensional manner is visualized in Fig. 3, based on the simulation findings. The left column represents the single seepage model, while the middle column illustrates the matrix flow in the dual seepage model. Lastly, the right column displays the preferential flow in the dual seepage model. For a more thorough analysis of seepage characteristics in different simulation conditions, it is vital to maintain uniformity in the initial simulation conditions and the saturation of the field soil across all simulations.

In the simulation process, the propagation of the wetting front in the single seepage model occurs parallel to the downward direction during both high-intensity irrigation and low-intensity irrigation. Upon reaching the saturated layer, the soil becomes saturated when the irrigation intensity is 25 mm/h. At an irrigation intensity of 2 mm/h, seepage takes place in an unsaturated condition. The dual seepage model's response to saturation demonstrates greater intricacy compared to the single seepage model, due to the interplay between matrix and preferential flows. When high-intensity irrigation is implemented, the irrigation intensity is 10.5 times greater than the saturated seepage coefficient of substrate flow in the dual seepage model. This leads to a linear increase in the effective saturation of matrix flow, reaching approximately 0.6. Following a time span of 28 hours, the groundwater level undergoes an increase, resulting in the saturation at a depth of 0.9 meters attaining a value of 1. Nevertheless, it is crucial to emphasize that the entirety of the area remains unsaturated, as indicated in Fig. 4(a). Concurrently, the effective saturation of the region influenced by the preferential flow wet front steadily rises until it reaches a value of 1, as depicted in Fig. 4(b).

Rapid infiltration of water into the deep layers and subsequent elevation of the groundwater level are attributed to the high saturated seepage coefficient of the preferential flow. The primary mode of water transfer in this context is from the preferential flow to the matrix flow, as shown in Fig. 4(e). The aforementioned statement elucidates that the upper layer of soil remains unsaturated, while the lower layer, known as the saturated layer, continues to experience an increase in moisture content. When low-intensity irrigation is employed, wherein the irrigation intensity is lower than the saturated seepage coefficient of the substrate flow, the water seepage is primarily governed by the flow of the substrate. As the wet front progresses towards the observation point, the saturation of the matrix flow swiftly reaches a value of 1 (Fig. 4(c)).

The findings suggest that the migration of matrix flow in this particular scenario is characterized by saturated migration, a phenomenon that contradicts the simulation outcome of the single permeability model. The effective saturation of the dominant watershed reaches approximately 0.6 after 100 hours and remains constant (Fig. 4(d)). It is evident that the dominant seepage process in this instance is unsaturated.

3.2 Water quality conversion characteristics

Through the analysis of water quality conversion features under diverse irrigation conditions (Fig. 5), it is observed that at an irrigation intensity of 25 mm/h, considered high intensity, the water seepage undergoes a transformation from preferential flow to matrix flow in all sectors, with the latter emerging as the dominant conduit. Infiltration of water into the matrix basin occurs as it diffuses and seeps through.

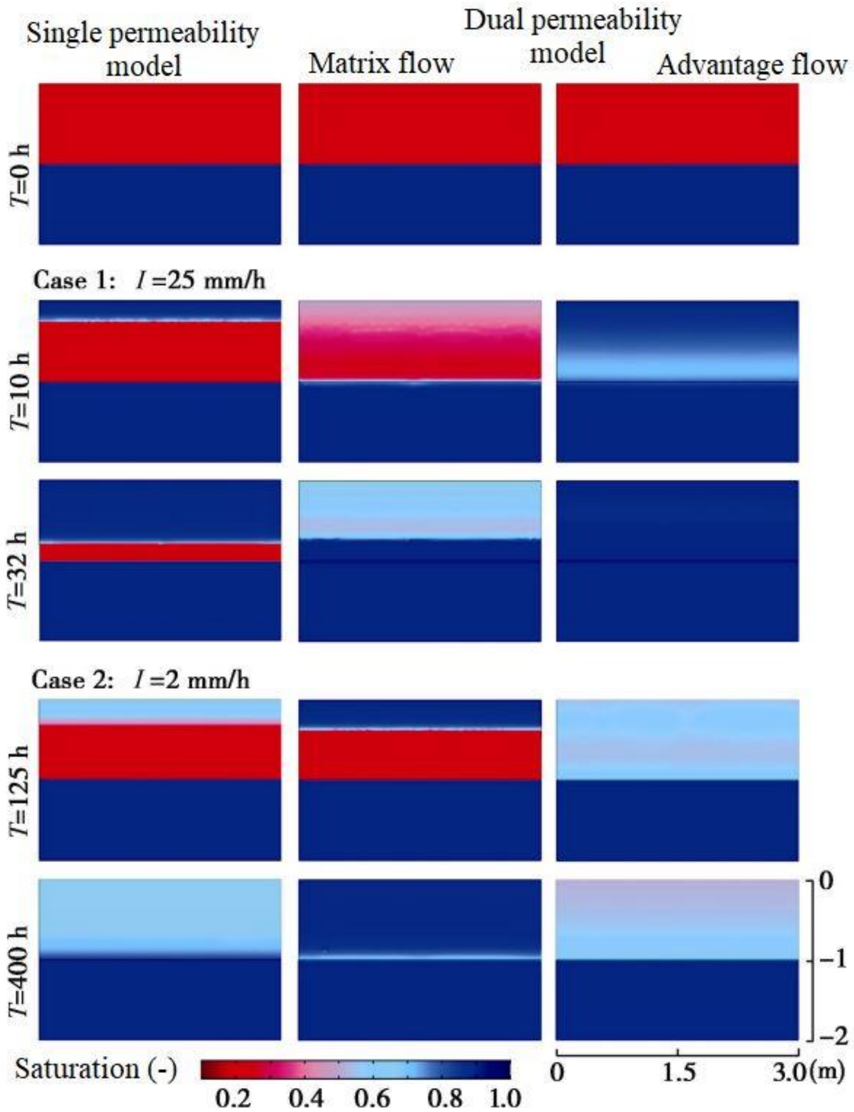

Figure 3 Saturation distribution by different models

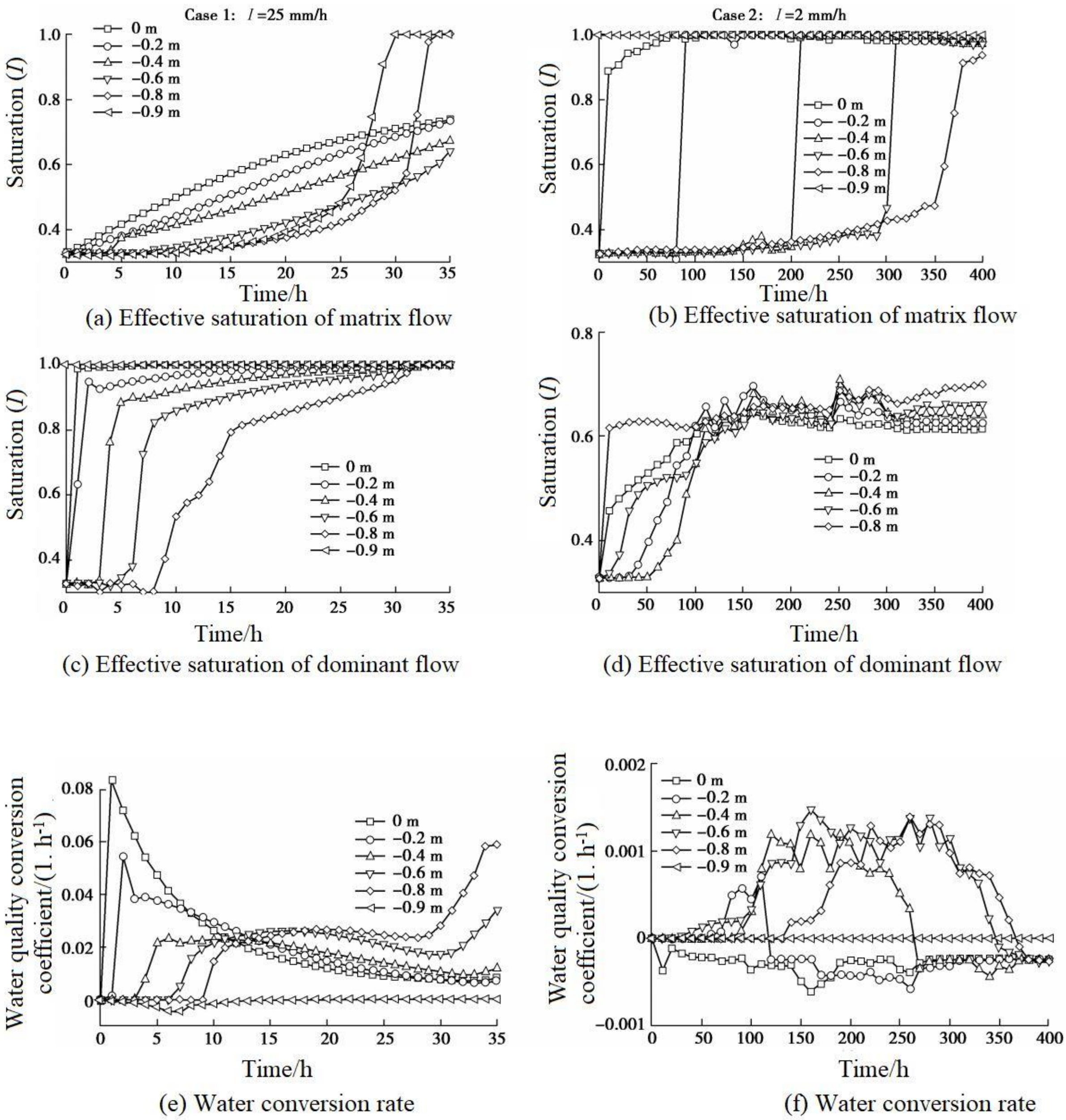

Figure 4 Saturations and water exchange rates by different models

(*Note: The flow from dominant flow to substrate flow is positive, and the flow from substrate flow to dominant flow is negative*)

The rapid preferential flow enables quick infiltration to the base, causing an elevation in groundwater levels. After 32 hours of seepage, the water level rises, with water quality conversion taking place only near the water level. When the irrigation intensity is set at 2 mm/h, indicating low intensity, the primary water exchange occurs from the substrate basin to the dominant basin. The presence of preferential flow results in a positive water exchange rate during the initial seepage phase. Upon reaching the observation depth, the seepage of the substrate undergoes a transition to negativity, signifying a shift from substrate flow to preferential flow of water. Following a duration of 350 hours, the entire area experiences a negative water exchange rate, indicating the movement of the matrix into the saturated layer.

According to the simulation results, the occurrence of preferential flow facilitates the rapid movement of high-intensity irrigation water towards the base of the slope through the dominant channel. Consequently, this leads to an elevation in the groundwater level, while the top layer of soil remains devoid of moisture. During this computational experiment, various models of infiltration were constructed to assess how preferential flow impacts the infiltration mechanism. It is crucial to acknowledge that the movement of water through soil is a complex phenomenon, and the concept of preferential flow is inherently subjective. Macro-pores and joints within the soil play a significant role as preferential seepage channels for water. Consequently, it is imperative to undertake further investigation and advancements in understanding the impact of preferential flow on the macro seepage process and the underlying mechanism.

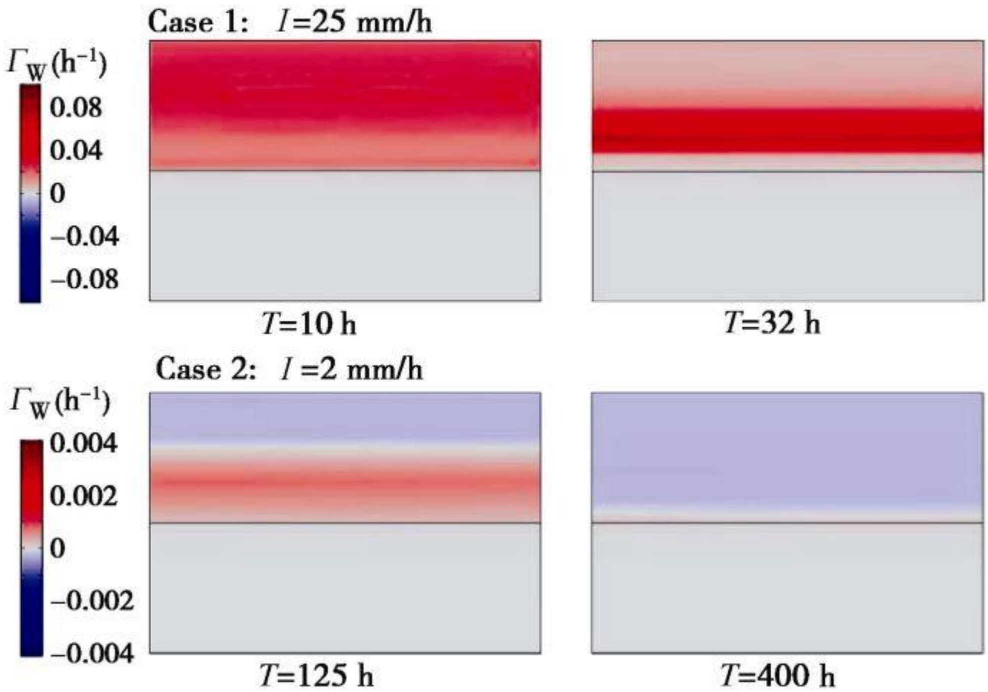

Figure 5 Distribution of water exchange rate

(Note: Red: dominant flow converted to matrix flow, Blue: matrix flow converted to dominant flow).

4. Conclusion

In this paper, the author delves into the development of characteristic cracks seen on loess plateaus and the process of water seepage that takes place on-site. Furthermore, the study conducts simulations to analyze the water seepage characteristics in the presence of preferential channels, ultimately leading to the formulation some distinct conclusions.

In the realm of numerical simulation, when faced with high irrigation intensity and a short duration, preferential flow assumes a dominant position. This phenomenon allows for the rapid infiltration of irrigation water to the lower layers, consequently leading to an increase in the groundwater level. The unsaturated top matrix flow exhibits high intensity during actual production. The concentrated irrigation or intense precipitation can easily infiltrate the bottom of the slope through preferential channels. In situations where irrigation intensity is low and duration is long, the matrix flow assumes a dominant role. Actual agricultural production may benefit from the utilization of unsaturated seepage, a method that entails prolonged irrigation periods and low irrigation intensity for optimal water conservation and efficiency.

Overall, this research contributes to the existing knowledge on loess plateau fractures and their relationship with water seepage. The findings enhance our understanding of the geological processes occurring in these regions and provide a foundation for future studies aimed at sustainable land management and hazard prevention.

Data Availability

The article provides the data used to support the results of this research.

Declaration of competing interest

No conflicts of interest to disclose.

References

P. Li. and Q. Hui, (2018) "Water in Loess," Encyclopedia of Sustainability Science and Technology, no. DOI: 10.1007/978-1-4939-2493-6_968-1, 2018.

P.Li, H. Qian, K. Howard and J. Wu,(2015) " Building a new and sustainable silk road economic belt," Environ Earth Sci, no. 74(10):7267–7270. https://doi.org/10.1007/s12665-015-4739-2, 2015. 2

E. Saibaba Reddy, K. Rama Sastri et K. Bhaskar ,(2010) «Filtering Decanting Water in Fly-Ash Lagoons Using Geotextiles — An Experimental Study,» Soil and Sediment Contamination: An International Journal, vol. 12, pp. 229-251, 2010.

W. Shao, T. Bogaard and M. Bakker,(2015) "Quantification of the influence of preferential flow on slope stability using a numerical modelling approach," Hydrol Earth Syst Sci , no. 19: 2197 – 2212, 2015.

I. Smalley, S. Marković and Z. Svirčev,(2011) "Loess is [almost totally formed by] the accumulation of dust," Quat Int, no. 240:4–11, 2011.

P. Garcia-Chevesich, X. Wei, J. Ticona and G. Martínez,(2020) "The Impact of Agricultural Irrigation on Landslide Triggering: A Review from Chinese, English, and Spanish Literature," Water, no. 10.3390/w13010010, 2020.

Y. Liang, J. Qiao and C. Xie, (2019) "The influence of the cracks on the landslide induced by irrigation: Take the southern Jingyang Plateau, Shaanxi Province as an example," Sci. Technol. Eng., no. 19, 305–314, 2019.

L. Zhu, J. Hu and J. Jia (2013) , "Development features and mechanical mechanism of irrigation-induced landslides in Heifangtai, Gansu Province," Geol. Bull. China , no. 32, 840–846, 2013.

J. Dong, (2017) "Study on the Trigger Mechanism and Motion Characteristics of Loess Landslide of Jingyang Village at South Jingyang Plateau," Master's Thesis, Department of Architecture and Civil Engineering, Xi'an, China, 2017.

J. Jia, L. Zhu and W. Hu (2013), "The formation mechanism and disaster mode of loess landslides induced by irrigation in Heifangtai, Gansu Province: A case study of the 13th landslide in Jiaojiayatou," Geol. Bull. China , no. 321968–1975, 2013.

Y. Dong, P. Sun, M. Zhang, X. Cheng and J. Bi,(2013) "The response of regional groundwater system to irrigation at Heifangtai terrace, Gansu Province," Geol. Bull. China , no. 32, 868–874, 2013.

M. Zhang,(2013) "Formation mechanism as well as prevention and controlling techniques of loess geo-hazards in irrigated areas: A case study of Heifangtai immigration area in the Three Gorges Reservoir of the Yellow River," Geol. Bull. China , no. 32, 833–839, 2013.

L. Xu, F. Dai, X. Tu, L. Tham, Y. Zhou and J. Iqbal,(2013) "Landslides in a loess platform, North-West China," Landslides , no. 11, 993–1005, 2013.

L. Xu, F. Dai, L. Tham, X. Tu, H. Min and Y. Zhou, (2011)"Field testing of irrigation effects on the stability of a cliff edge in loess , North-west China," Eng. Geol. , no. 120, 10–17, 2011.

G.-C. Pablo , W. Xiaolu , T. Juana , M. Gisella , Z. Julia , . G. Vilma, A. Francisco , Z. Yao , F. Hanna , G. Andrew , S. Paul , M. John , G. Edgard et K. Richard (2021), «The Impact of Agricultural Irrigation on Landslide Triggering: A Review from Chinese, English, and Spanish Literature,» Water , 2021.

T. Gu, M. Zhang, J. Wang, C. Wang, Y. Xu and X. Wang,(2018) "The effect of irrigation on slope stability in the Heifangtai Platform, Gansu Province, China," Eng. Geol., pp. 248, 346–356, 2018.

W. Wu, X. Su and X. Meng,(2014) "Characteristics and origin of loess landslides on loess terraces at Heifangtai, Gansu Province, China," Appl. Mech. Mater, pp. 694, 455–461, 2014.

X. Hou, S. Vanapalli and T. Li (2018), "Water infiltration characteristics in loess associated with irrigation activities and its influence on the slope stability in Heifangtai loess highland," China. J. Eng. Geol, pp. 234, 27–37, 2018.

Z. Duan, W. Cheng, J. Peng, Q. Wang and W. Chen (2019), "Investigation into the triggering mechanism of loess landslides in the south Jingyang platform, Shaanxi province," Bull. Eng. Geol. Environ., pp. 78, 4919–4930, 2019.

H. Li and Y. Jin (2012), "Initiation analysis of an irrigation-induced loess landslide," Appl. Mech. Mater , pp. 170–173, 574580, 2012.

T. Gu, L. Zhu, W. Hu, J. Wang and Y. Liu (2015) , "Effect on slope stability due to groundwater rising caused by irrigation: A case study of Heifang Platform in Gansu," China Geosci, pp. 29, 408–413, 2015.

B. Zhou and Z. Chen(2019), " Effects of density and hysteresis on hydraulic conductivity function of compacted expansive soil," Chinese Journal of Geotechnical Engineering, no. 41(10): 1800–1808, 2019.

H. Hu (2018), "Study on the method for determining the unsaturated permeability coefficient of loess in humidification," Journal of Hydraulic Engineering, no. 49(10): 1216–1226, 2018.

B. Hong, X. Li and G. Chen(2016), "Experimental study of permeability of remolded Malan loess," Journal of Engineering Geology, no. 24(2): 276–283, 2016.

T. Wang, T. Yang and J. Lu (2016), "Influence of dry density and freezing-thawing cycles on anisotropic permeability of loess," Rock and Soil Mechanics, no. 37(S1): 72–78, 2016.

K. Zhao, Q. Xu and X. Zhang (2018), "The research on the infiltration characteristics in the topsoil of Heifangtai in Gansu Province," Engineering Geology, no. 26(2): 459–466., 2018.

J. Lu and and B. Chen (2007), "Research on soil-water characteristic curve of unsaturated loess," Chinese Journal of Geotechnical Engineering, no. 29(10): 1591–1592, 2007.

T. Wang, N. Li and D. Xie (2004), "GravitationaI potential， matrix suction and thermal potentiaI of unsaturated loess soil," Chinese Journal of Geotechnical Engineering, no. 26(5): 715–718, 2004.

P. Li, T. Li and A. Wang (2013) , "Field experimental study on the law of water migration in loess," Rock and Soil Mechanics, no. 34(5): 1331–1339, 2013.

Q. Mu, Y. Dang and Q. Dong (2019), "Water-retention characteristics and collapsibity behaviors: comparison between intact and compacted loesses," Chinese Journal of Geotechnical Engineering, 2019.

L. Xu, H. Li and D. Wu(2008) , "Discussion on infiltration of surface water and their significance to terrace loess landslides," Chinese Journal of Geological Hazard and Control, no. 19(2): 32–35, 2008.

T. Wang (2008) , "Moisture migration in unsaturated loess subgrade," Chinese Journal of Geotechnical Engineering , no. 30(1): 41 –45, 2008.

Y. Liang(2011), "Numerical simulation model for pore flows and distribution of their velocity," Chinese Journal of Geotechnical Engineering, no. 33(7): 1104–1109, 2011.

A. Zhang, S. Kang and P. Li(2004), "3D seepage numerical analysis of three-dimensional drainage system in loess landsliding body," Soil and Water Conservation Bulletin, no. 24(6): 6–9, 2004.

P. Sun, M. Zhang and Y. Dong (2013), " The coupled analysis of phreafic water flow and slope stability at Heifangtal terrace Gansu Province," Geological Bulletin of China, no. 32(6): 887–892, 2013.

Y. Liang, P. Chen and J. Lin (2019), "Pore flow characteristics of porous media based on transparent soil technology," Chinese Journal of Geotechnical Engineering, no. 41(7): 1361–1366, 2019.

T. Vogel, H. Gerke and R. Zhang (2000), " Modeling flow and transport in a two-dimensional dual-permeability system with spatially variable hydraulic properties," J Hydrol, no. 238: 78–89, 2000.

H. Gerke. and M.Genuchten(1993), "A dual porosity model for simulating the preferential movement of water and solutes in structured porous media," Water Resour. Res, pp. 29, 305–319,1993a., 1993.

C. Ray, T. Ellsworth and A. Valocchi (1997), " An improved dual porosity model for chemical transport in macroporous soils," J Hydrol, p. 193: 270–292, 1997.

B. Arora, B. Mohanty and J. Mcguire (2011) , "Inverse estimation of parameters for multidomain flow models in soil columns with different macropore densities," Water Resour Res, pp. 47, W04512, doi:10.1029/2010WR009451., 2011.

H. Laine-kaulio, S. Backnas and T.Karvonen (2014) , "Lateral subsurface stormflow and solute transport in a forested hillslope: a combined measurement and modeling approach," Water Resour Res , p. 50: 8159–8178, 2014.

R. B. a. A. Corey (1964), "Hydraulic Properties of Porous Media," Colorado State University, Colorado, 1964.

S. Wei , B. Thom , S. Ye et . B. Mark (2016) , «Coupling a 1D Dual-permeability Model with an Infinite Slope Stability Approach to Quantify the Influence of Preferential Flow on Slope Stability,» Procedia Earth and Planetary Science, vol. 16, pp. 128-136, 2016.

Received: December 10 2023
Accepted : January 07 2024